

# Polyphase deformation in Oscar II Land, central western Svalbard

ALAN MORRIS



Morris, A. 1988: Polyphase deformation in Oscar II Land, central western Svalbard. *Polar Research* 6, 69–84.

Pre-Carboniferous rocks in central western Svalbard can be divided into two rock packages that have experienced three phases of deformation. The lower package includes upper Proterozoic sediments, the upper package is of upper Ordovician to lower Silurian age. Pre-upper Ordovician (Caledonian) deformation is characterized by north-south fold-axes, and is recorded in the lower package only. Following the Ordovician, east-west fold axes developed in the upper package but only locally in the lower. The third phase, probably Tertiary in age, produced easterly directed thrusting, and refolding about sub-horizontal, north-south fold axes in both packages. This complex structural history has resulted in tectonic thickening of the rock sequences by refolding and thrusting which has not been recognized by previous workers.

*Alan Morris, Division of Earth and Physical Sciences, University of Texas, San Antonio, Texas 78285-0663, U.S.A.; December 1986 (revised December 1987).*

The pre-Carboniferous sequence of Oscar II Land has been involved in two major orogenic events, one Caledonian and the other Tertiary in age (Harland & Horsfield 1974; Hjelle et al. 1979; Kowallis & Craddock 1984; Birkenmajer 1981) (Fig. 1). Two rock packages, an upper and a lower, are distinguished both sedimentologically and structurally (Weiss 1953; Hjelle et al. 1979; Harland et al. 1979; Ohta et al. 1984). Despite the lack of fossils and radiometric age data, diamictite horizons (Haaken Formation) within the lower package are correlated with the Varangian tillites of northern Norway (Hambrey 1983), and upper Ordovician to lower Silurian fossils are found within the upper package (Scrutton et al. 1976; Armstrong et al. 1986). The lower package has previously been regarded as a more or less homoclinal, west-dipping, west-younging sequence (Harland et al. 1979; Waddams 1983), although it contains thrust slices of exotic, high-pressure blueschists (Horsfield 1972; Hjelle et al. 1979; Ohta 1979; Ohta et al. 1986).

The St. Jonsfjorden area of Oscar II Land has been recognized as structurally complex (Hjelle et al. 1979; Waddams 1983), and most workers have preferred to base their stratigraphic schemes in areas where rock sequences are thought to be more complete and less complicated (e.g. Waddams 1983). Detailed mapping in central western Oscar II Land has now established a

stratigraphic scheme for the area, the results of which are published elsewhere (Kanat & Morris 1988). Here I present a new view of the structural geology of the St. Jonsfjorden area, based on the same field work, which allows the geometrical effects of three deformation phases to be determined. These results illustrate that the development and intensity of deformation features vary considerably with stratigraphic unit. In addition, alternations of lithology previously thought to have been sedimentary transition sequences can be shown to be the results of superposed fold interference patterns.

## Structural terminology

Bedding, cleavage and crenulation cleavage are referred to as S-surfaces (Turner & Weiss 1963), subscripted to denote primary layering ( $S_0$ ) and relative chronology of formation ( $S_1$ ,  $S_2$ ). Bedding-cleavage intersection lineations and fold axes are denoted L and subscripted as for S-surfaces. Folds of different generations are referred to as  $F_1$  and  $F_2$ . Letter subscripts are added to denote lower (a) and upper (b) package.

Minor fold and cleavage vergence are recorded as S, Z, or M when viewed down the plunge of the fold axis or bedding-cleavage intersection lineation (Ramsay 1967). Major fold vergence is defined as the sense of overturning of a fold, up

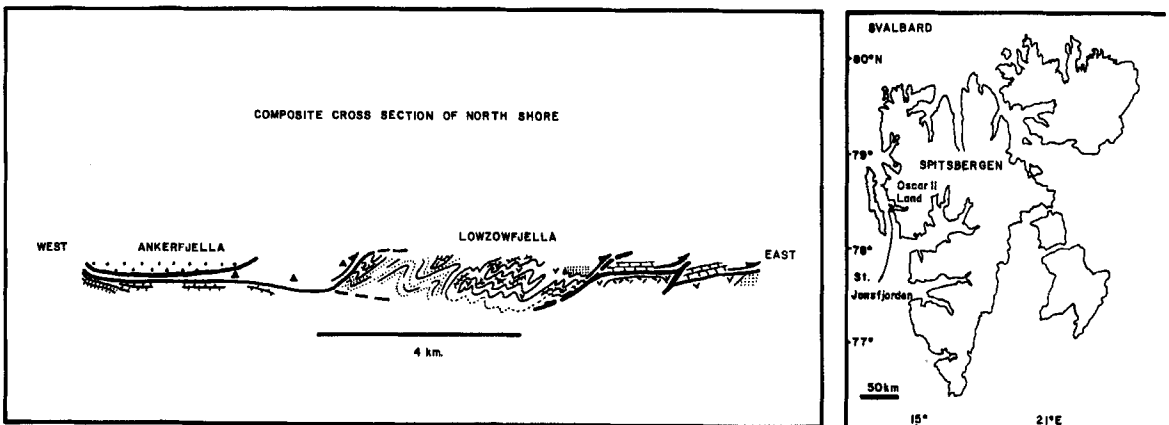
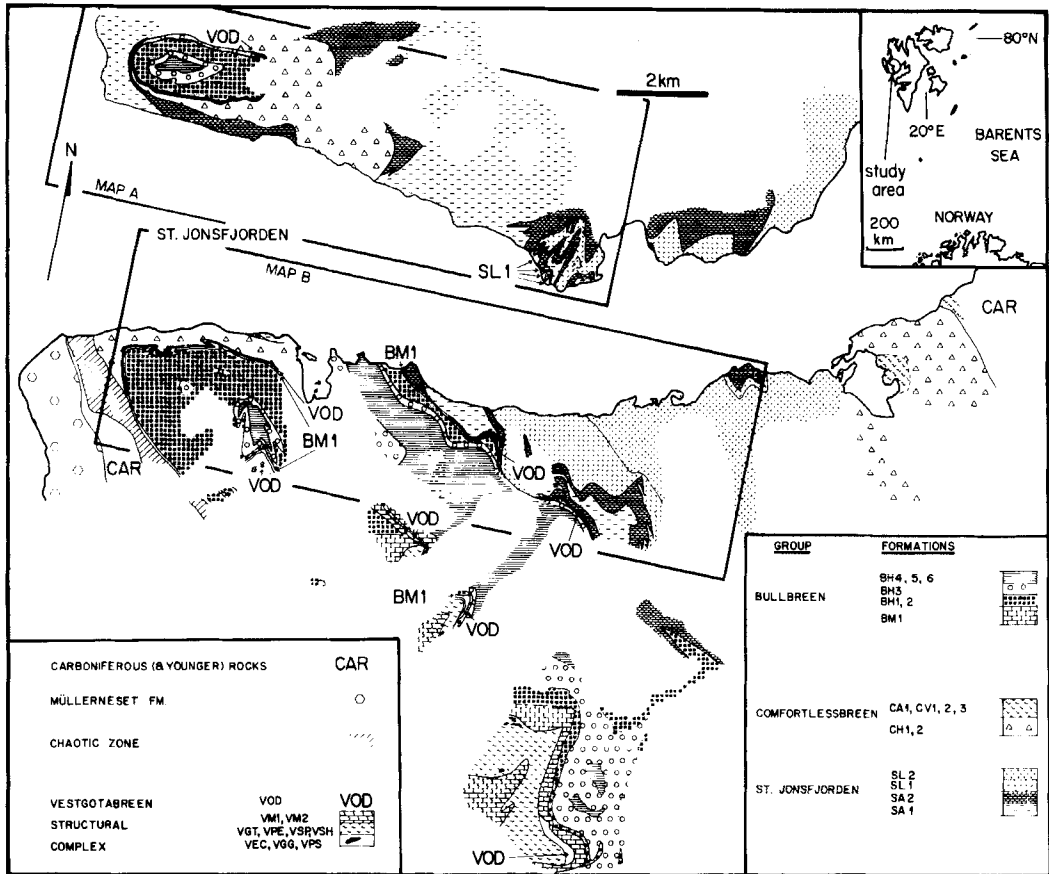
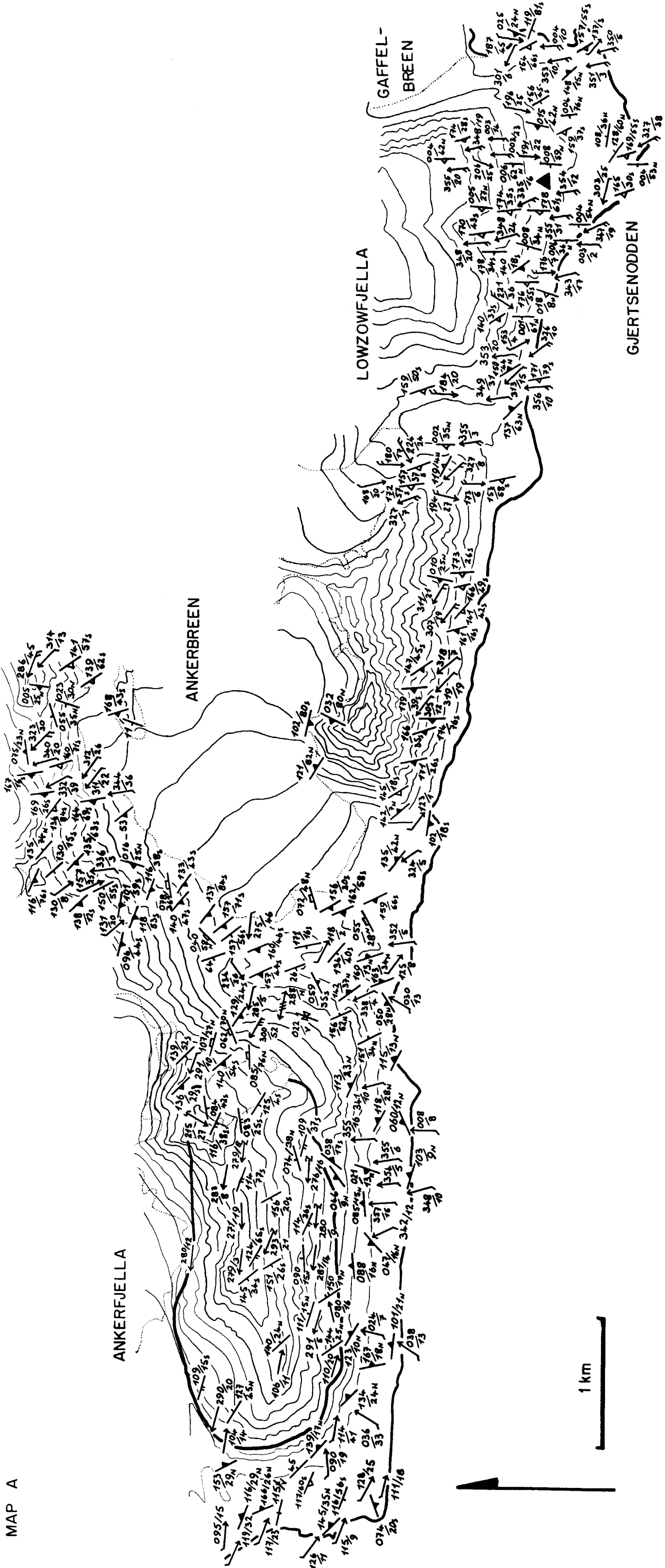


Fig. 1. Location map and cross section, geological map of the St. Jonsfjorden area (from Kanat & Morris 1988); maps A and B are detail maps showing selected field data. Location X is shown as a filled triangle on map A and location Y is shown as a filled circle on map B. More detailed maps can be obtained from the author.

MAP A



MAP B

KEY TO MAPS A & B

UPPER PACKAGE

S<sub>0b</sub> S<sub>1b</sub>

L<sub>1b</sub>

kinks

LOWER PACKAGE

S<sub>0a</sub>

S<sub>1a</sub>

S<sub>2a</sub>

S<sub>3a</sub>

L<sub>1a</sub>

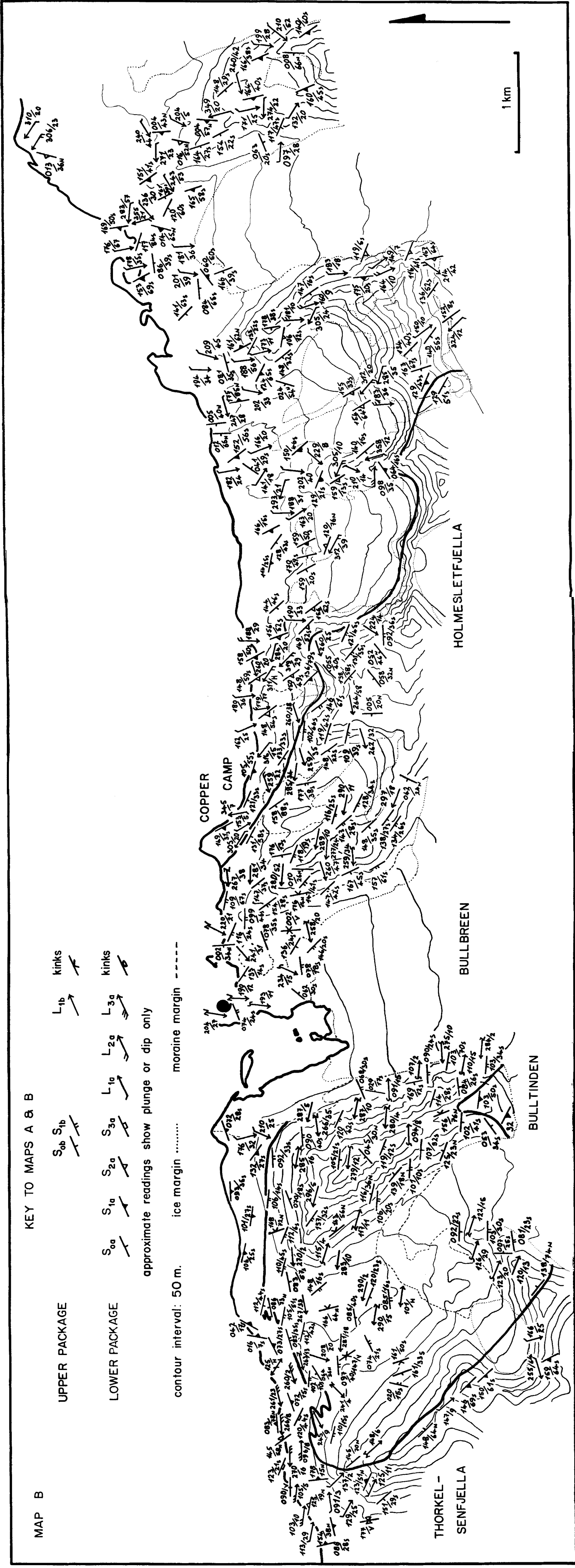
L<sub>2a</sub>

L<sub>3a</sub>

kinks

approximate readings show plunge or dip only

contour interval: 50 m. ice margin ..... moraine margin -----



the dip of the axial surface (Bell 1981). Facing is the younging direction on a cleavage surface perpendicular to the bedding-cleavage intersection lineation (Shackleton 1957).

## Metamorphic grade

Quartz, calcite, white mica and chlorite are the most common metamorphic minerals in the psammitic and pelitic rocks of both packages. They occur along cleavage planes, in crack-seal veins, or as overgrowths on competent grains. There is no evidence for retrograde metamorphism.

## Structural fabric elements

### *Lower package*

Bedding,  $S_{0a}$ , is visible in exposures of the sandstone-phyllite of the Alkhorn Formation and quartzite-slate unit of the Løvliebreen Formation, but only locally distinguishable in the Haaken Formation and very rarely in the Alkhorn Limestone and volcanic unit of the Løvliebreen Formation. In thin-section it is most commonly manifest as a grain-size and mica-content variation (Figs. 2D, F and J) and less commonly as a concentration of opaque minerals. In some cases  $S_{0a}$  can only be recognized by its effect on  $S_{1a}$ , either refracting  $S_{1a}$  or causing a variation in its development (Fig. 2D).  $S_{1a}$  is the dominant fabric visible in the exposure, with an associated bedding-cleavage intersection lineation ( $L_{1a}$ ) manifest as a texture and colour variation on  $S_{1a}$  surfaces. Tight ( $F_{1a}$ ) folds have axes parallel to  $L_{1a}$ .

$S_{1a}$  is usually present as anastomosing seams of pressure-insoluble material (carbon, iron-sulphide and mica, Fig. 2E). Other evidence for pressure-solution includes truncated grains and ooids (Figs. 2F and G), and fibrous overgrowths of quartz, calcite and chlorite on high-competence grains (Figs. 2A and L). Micro-cracks at high angles to the maximum extension direction (as indicated by fibre long-axes) are common in large clastic grains and lithic fragments (Figs. 2A and B), crack-seal veinlets occur in the Løvliebreen quartzite-slate unit (Fig. 2H) and selvages of white mica occur in the Haaken diamictite unit (Fig. 2C). In some carbonate horizons in the Alkhorn Formation extension has been accom-

modated by 'tearing' of the rock along irregular fractures with no apparent relationship to pre-existing structures. In these cases the maximum extension direction is indicated by fibrous growths of calcite and is sub-parallel to  $S_{1a}$  traces (Fig. 2G). Stress-induced recrystallization of large quartz grains is evident in silici-clastic rocks (Fig. 2I).

An extensional crenulation cleavage (Platt & Vissers 1980) is developed at some localities (Fig. 2L). It clearly post-dates the main cleavage ( $S_{1a}$ ), but cannot be designated  $S_{2a}$  because fibre growths associated with the feature are sub-parallel to  $S_{1a}$  traces, and the minimum and maximum extension directions inferred from its geometry indicate that it may be a late-stage variant of  $S_{1a}$ .

$S_{2a}$  can be distinguished in Løvliebreen volcanic and Haaken diamictite units as a compressional crenulation cleavage (Figs. 2C and 3B). In other units it is quasi-penetrative, morphologically identical to  $S_{1a}$  and axial planar to close to tight folds (Fig. 3A). Here, it can only be identified with confidence in or near  $F_{2a}$  hinges (Fig. 2K). Fig. 2J shows how  $S_{2a}$  can be recognized by comparing vergence senses of cleavage traces in refolded folds when the fold generations are known. It is also possible to identify  $S_{2a}$  by following  $S_{1a}$  traces from  $F_{1a}$  folds into  $F_{2a}$  folds (Fig. 2K). However,  $S_{1a}$  and  $S_{2a}$  cannot be distinguished where the two fold phases are not visible together.

In the western sub-areas, poles to  $S_{1a}$  show girdle distributions indicating refolding about NW to SE or WNW to ESE, sub-horizontal fold axes (sub-areas A, C2 and C3, Fig. 4), whereas in the east they show point maxima or refolding about NS, subhorizontal axes (sub-areas B, D and E, Fig. 4). At the western edge of the outcrop  $S_{1a}$  dips steeply to the NE (sub-areas A and C1, Fig. 4) and  $L_{1a}$  orientations depart from the patterns prevalent to the east. In addition, the western areas have open upright folds with sub-horizontal NS axes which deform  $S_{0a}$ ,  $S_{1a}$  and  $L_{1a}$ .

Refolding of  $S_{0a}$ ,  $S_{1a}$  and  $L_{1a}$  at a mesoscopic scale is more conspicuous further east.  $F_{2a}$  axes have approximately NS, sub-horizontal orientations and make angles of 10–15° with  $F_{1a}$  axes (Fig. 3A).  $S_{2a}$  dips moderately to steeply WSW and poles to  $S_{1a}$  have girdle distributions indicating folding about the  $F_{2a}$  axes (sub-areas B, D and E, Fig. 4). At some localities,  $L_{1a}$  and  $F_{1a}$  axes are folded within an undeviated  $S_{1a}$  plane (e.g. Ramsay 1967). Deformed  $L_{1a}$  lineations form a broad, WSW dipping girdle (sub-areas B,

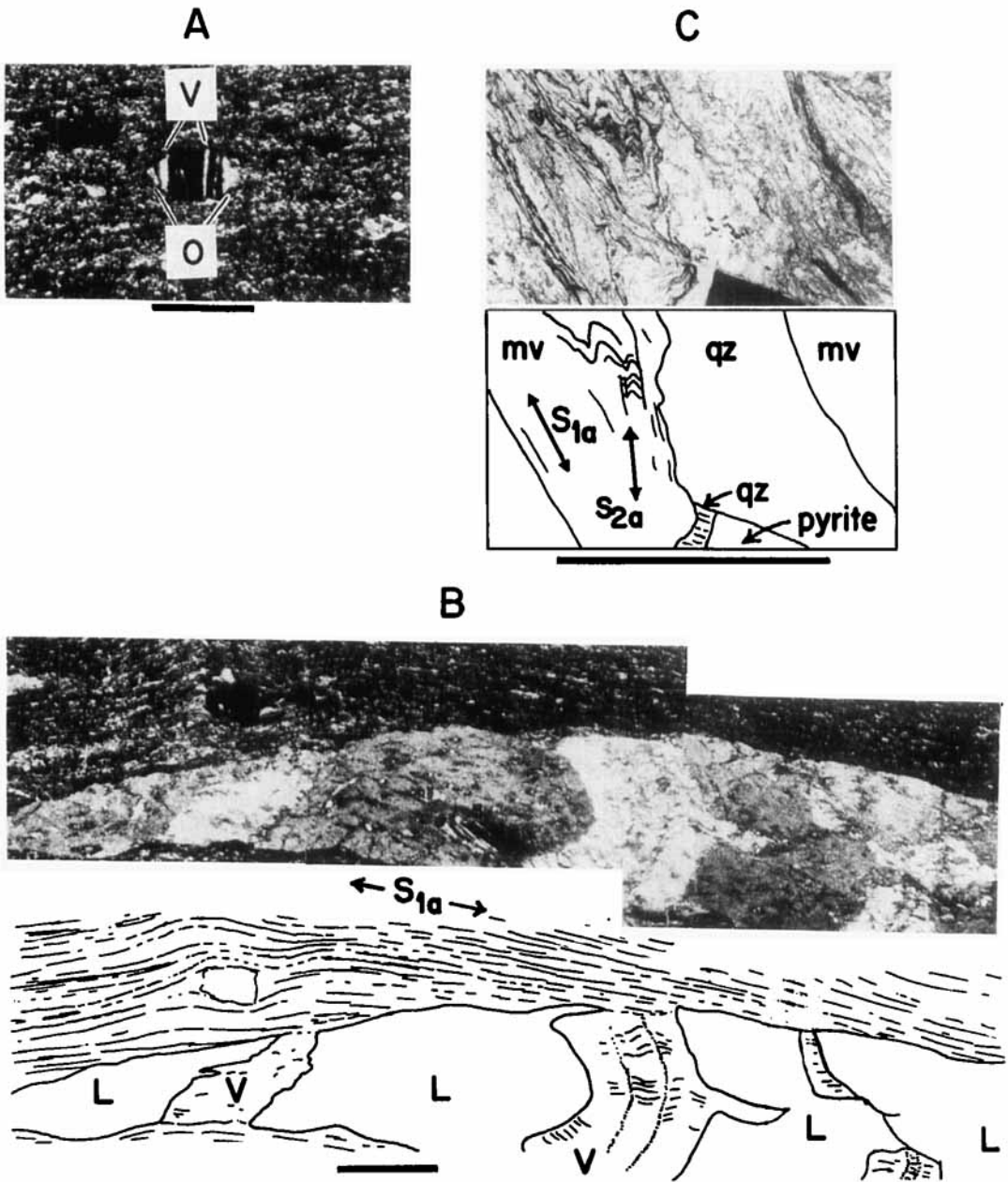


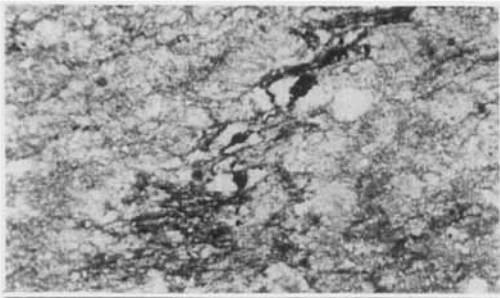
Fig. 2. Microscopic structural fabric elements in the lower package. Scale bars are 1 mm in length, PPL denotes plane polarized light, XPL denotes crossed polarizer and analyser; details of localities can be obtained from the author.

A. Løvliebreen Fm. (SL1), south shore, M3741A XPL. Photomicrograph of stretched feldspar grain with calcite-filled veinlets (V) and overgrowths (O) that have formed at a high angle to the extension direction, contained with  $S_{1a}$ . The trace of  $S_{2a}$  is parallel to the scale bar.

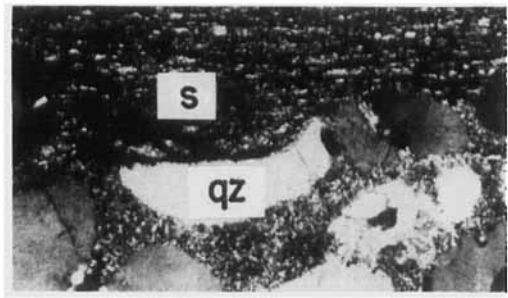
B. Løvliebreen Fm. (SL1), south shore, M3741B XPL. Sketch and photomicrograph to show stretched lithic fragment (L) cut by calcite filled veins (V). The veins have inclusion trails indicating that they are crack-seal in nature. Sigmoidal form of some fibres may be attributable to later cleavage-parallel compression because other parts of this thin section exhibit compressional crenulation cleavage. Note that the trace of  $S_{1a}$  is slightly oblique to the margins of the lithic fragment, indicating that some component of the grain shape is primary and not entirely tectonic.

C. Haaken Fm. (CH1), south shore, M3597A PPL. Sketch and photomicrograph to show white mica (mv) and quartz (qz) rich domains delineating  $S_{1a}$ .  $F_{2a}$  microfolds cause  $S_{2a}$  which crosscuts pre-existing features including quartz fibre growths on the pyrite grain.

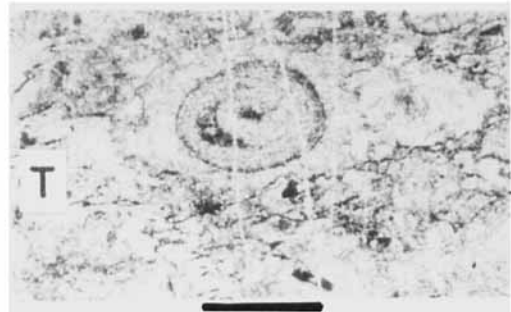
D



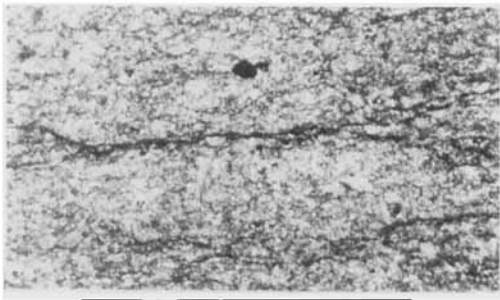
F



G



E



H



D. Alkhorn Fm. (SA1), north shore, G071A PPL. Sketch and photomicrograph showing  $S_{0a}$  delineated by a thin lamina of mica and carbonate rich material (C) within a more quartzose lithology (qz). The development of  $S_{1a}$  is stronger in lamina C than in the surrounding lithology. It is also slightly refracted through the lamina.

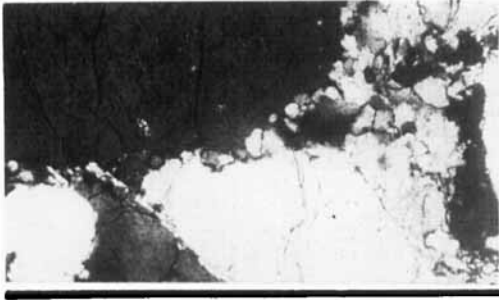
E. Løvliebreen Fm. (SL1), south shore, M3739 PPL. Photomicrograph of anastomosing and branching pressure solution cleavage planes.  $S_{1a}$  trace is approximately parallel to the scale bar.

F. Løvliebreen Fm. (SL2), north shore, M3728 XPL. Photomicrograph of quartz grain (qz) in sandstone layer pressure-solving against slaty, mica rich material (S).  $S_{1a}$  trace is parallel to the scale bar.

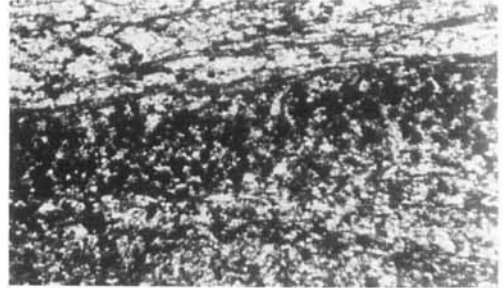
G. Løvliebreen Fm. (SL2), south shore, M3737B PPL. Photomicrograph of ooid surrounded by pressure solution seams, and fibrous quartz and calcite growth developing a 'tearing' fabric (T).  $S_{1a}$  trace is parallel to the scale bar.

H. Løvliebreen Fm. (SL2), north shore, M3718 XPL. Photomicrograph of calcite- and quartz-filled crack-seal vein in lithic fragment. Quartz grains in the matrix have quartz and sericite overgrowths (circled).  $S_{1a}$  trace is parallel to the scale bar.

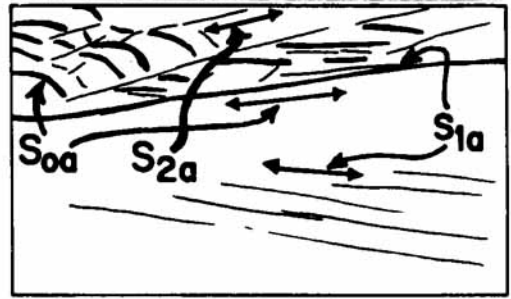
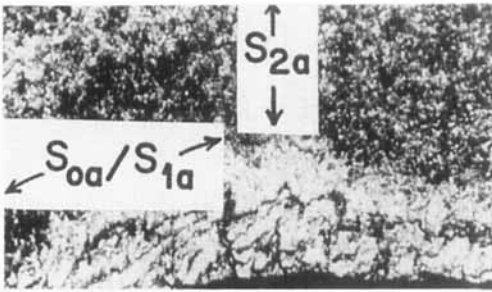
I



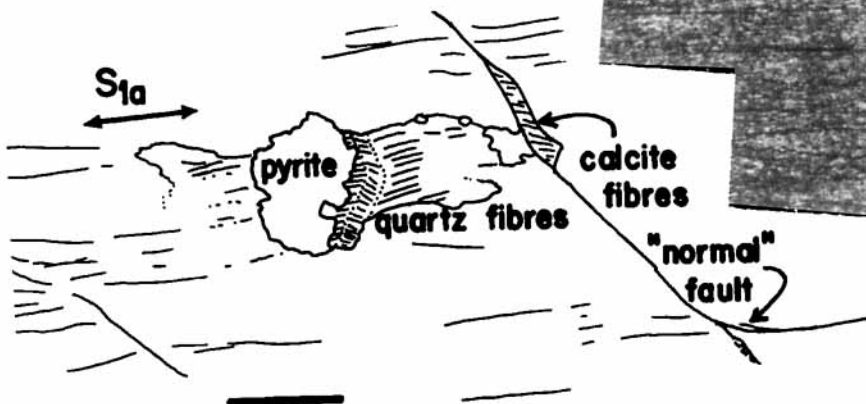
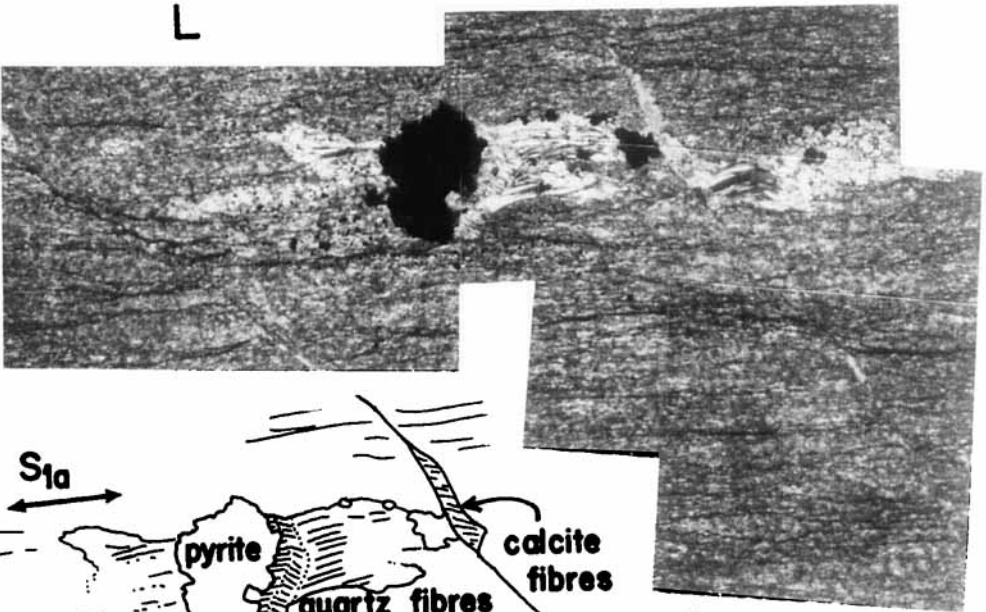
J



K



L



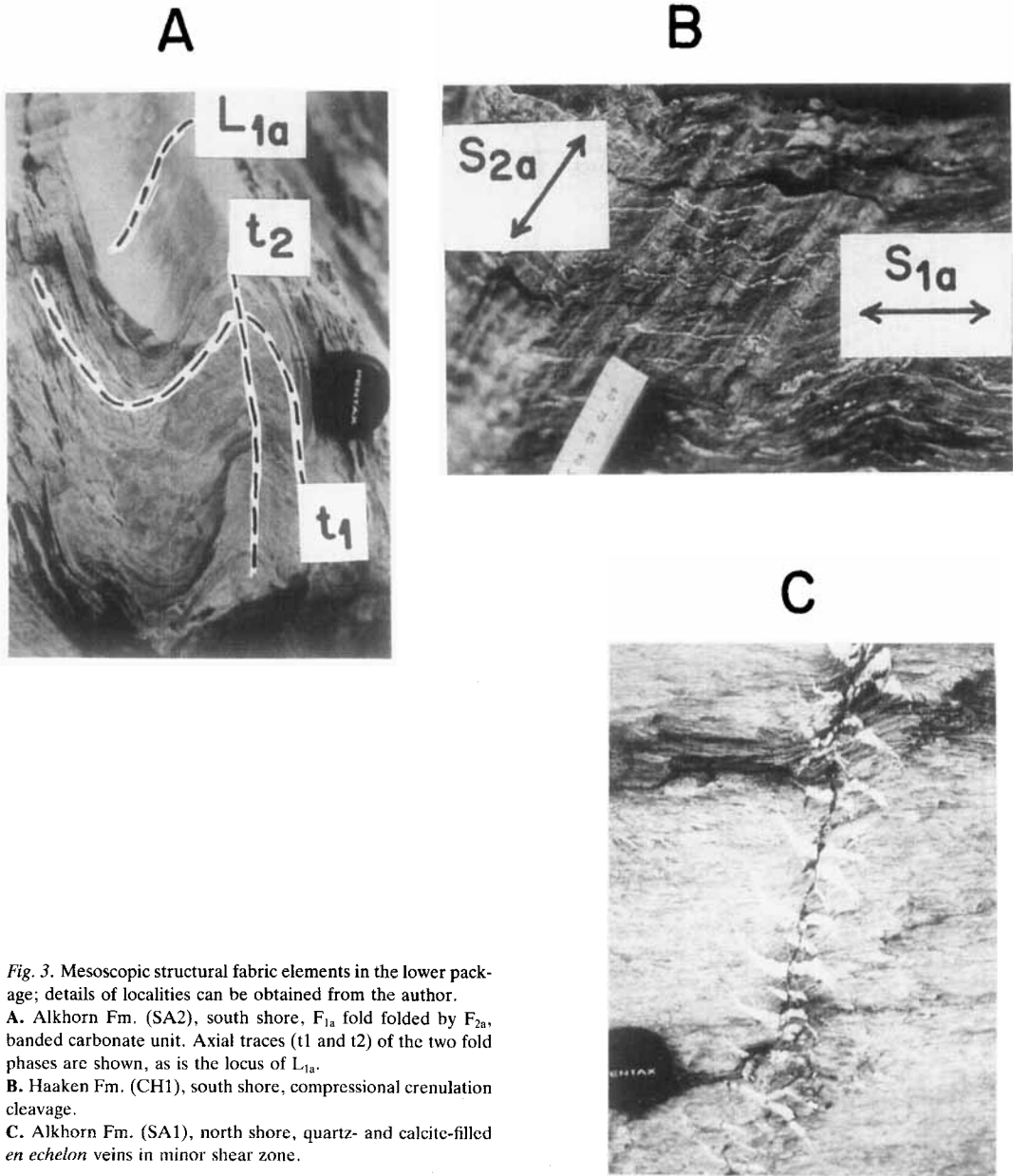


Fig. 3. Mesoscopic structural fabric elements in the lower package; details of localities can be obtained from the author.

**A.** Alkhorn Fm. (SA2), south shore,  $F_{1a}$  fold folded by  $F_{2a}$ , banded carbonate unit. Axial traces ( $t_1$  and  $t_2$ ) of the two fold phases are shown, as is the locus of  $L_{1a}$ .

**B.** Haaken Fm. (CH1), south shore, compressional crenulation cleavage.

**C.** Alkhorn Fm. (SA1), north shore, quartz- and calcite-filled *en echelon* veins in minor shear zone.

**I.** Løvliebreen Fm. (SL2), south shore, M3708 XPL. Photomicrograph of stress-induced grain size diminution at quartz/quartz-grain contacts.  $S_{1a}$  trace is parallel to the scale bar.

**J.** Alkhorn Fm. (SA1), south shore, M3704B XPL. Sketch and photomicrograph. The thin section is almost parallel to  $F_{1a}$ , oblique to  $F_{2a}$  and perpendicular to  $S_{2a}$ . Note that the vergence sense of the  $S_{2a}$  traces in the upper part of the photograph is opposite to that of the  $S_{1a}$  traces in both the upper and lower parts of the photograph.

**K.** Alkhorn Fm. (SA1), south shore, M3704A XPL. Photomicrograph. Note that the  $S_2$  traces are strongest in the hinge region of the fold, and they die out rapidly away from this area.

**L.** Alkhorn Fm. (SA2), north shore, M3739A XPL. Sketch and photomicrograph showing quartz fibre growths on pyrite grains and in dilational areas associated with a late first phase extensional crenulation cleavage.

D and E, Fig. 4). The locus of deformed  $L_{1a}$  lineations for each  $F_{2a}$  fold, however, defines a great circle girdle which is unique to that fold.

At locality X (filled triangle, Map A, Fig. 1),

west and north of Gjertsenodden, 20–30 mm half-wavelength minor folds are exposed exhibiting anomalous vergence on one limb of a 10–15 m half-wavelength fold, indicating refolding of

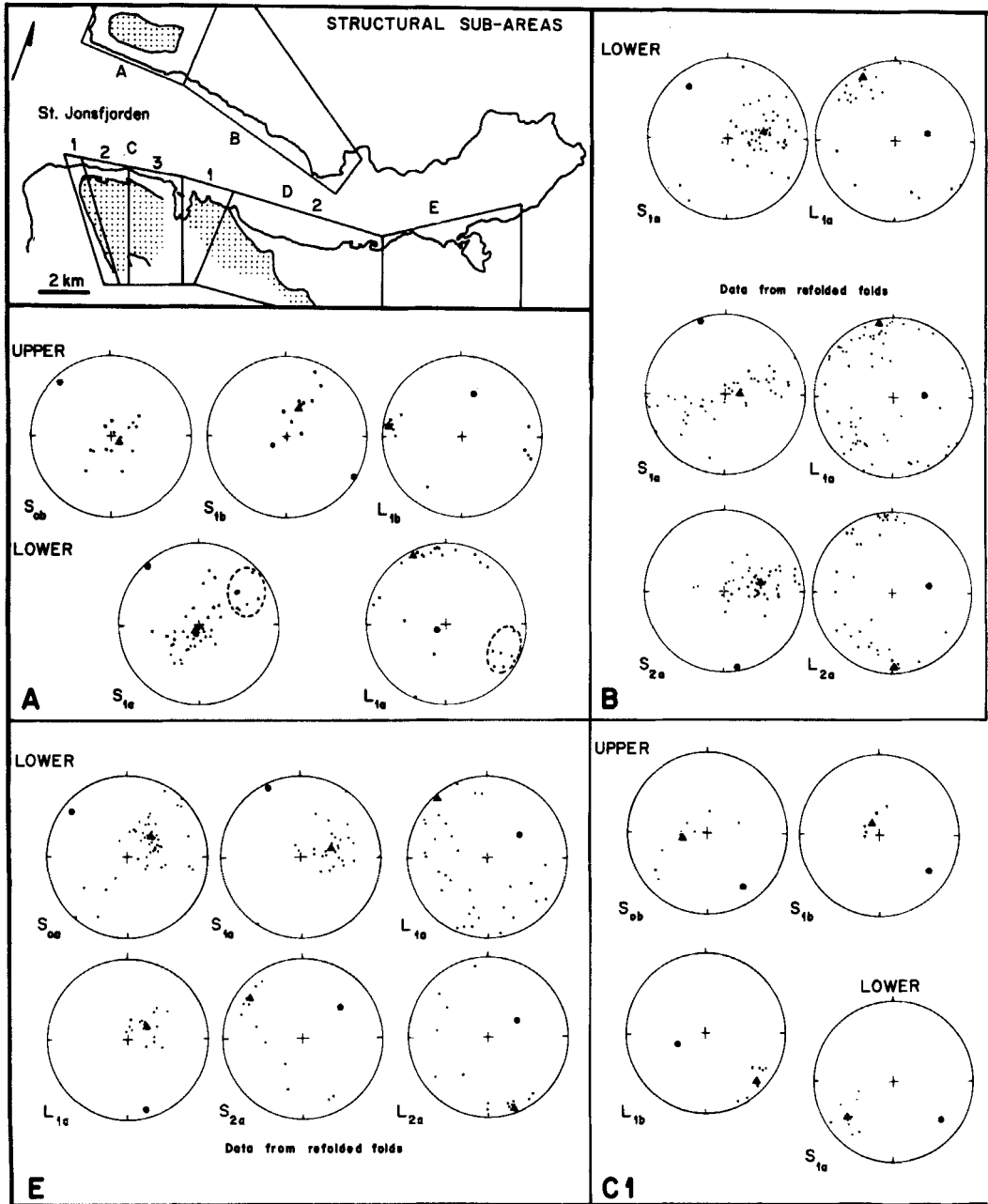
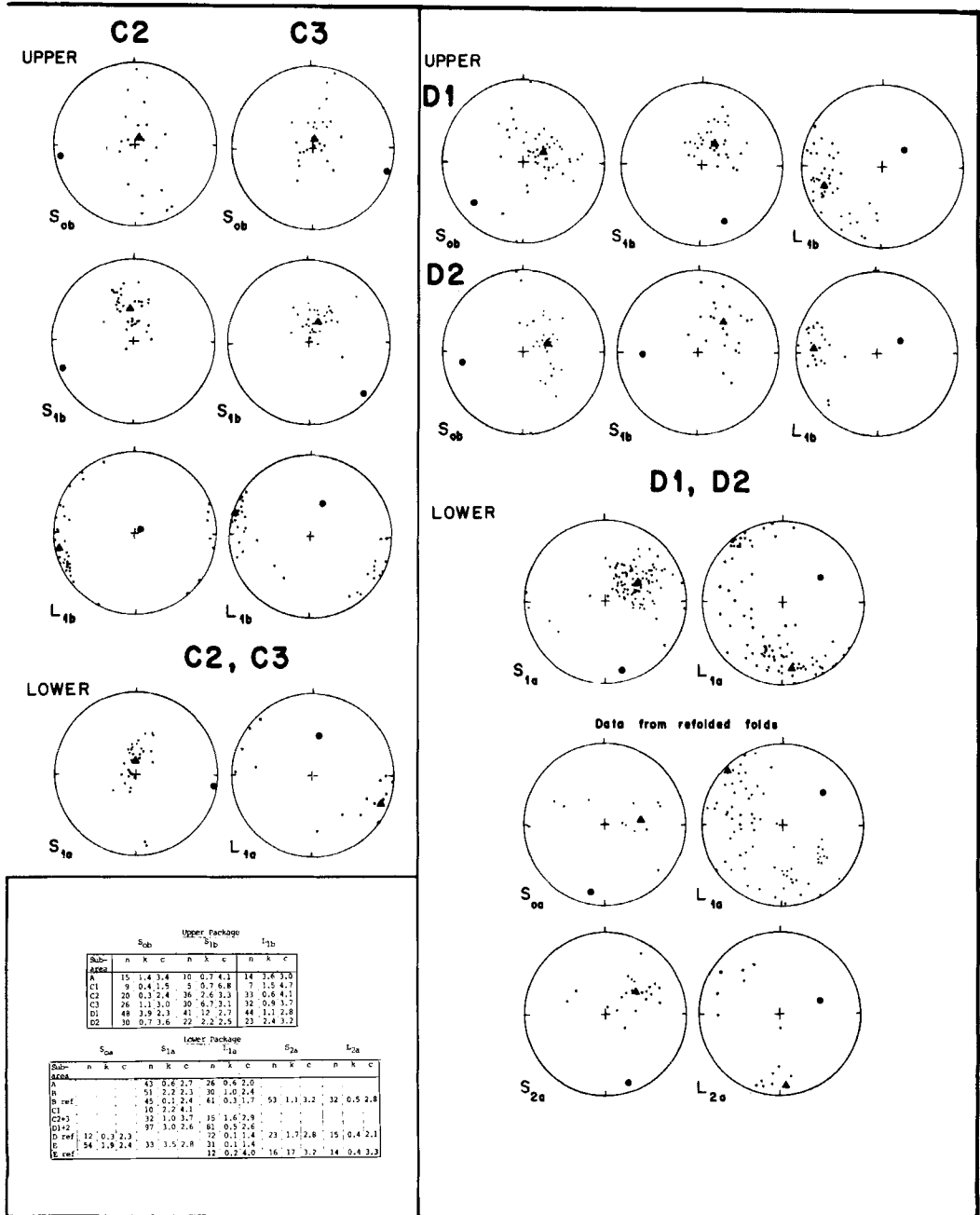


Fig. 4. Map of St. Jonsfjorden showing structural sub-areas, stippled pattern shows outcrop area of the upper package, with lower hemisphere, equal-area projections of field data by sub-area. Planar fabrics are represented by poles ('pi-plots'). Statistical data for these distributions are given in the table: n = number of points, k > 1 indicates a cluster, k < 1 indicates a girdle, c indicates the strength of the preferred orientation (Woodcock & Naylor 1983), ref indicates data from refolded folds only.

earlier structures. Both  $F_{1a}$  and  $F_{2a}$  folds are overturned towards the east.

Small, sub-vertical NNW to SSE trending shear zones containing calcite *en echelon* tension veins

occur in the zone of conspicuous refolding (Fig. 3C). These zones deform  $S_{1a}$  but their relationship with  $S_{2a}$  is unknown. Sense of displacement is variable from shear zone to shear zone.



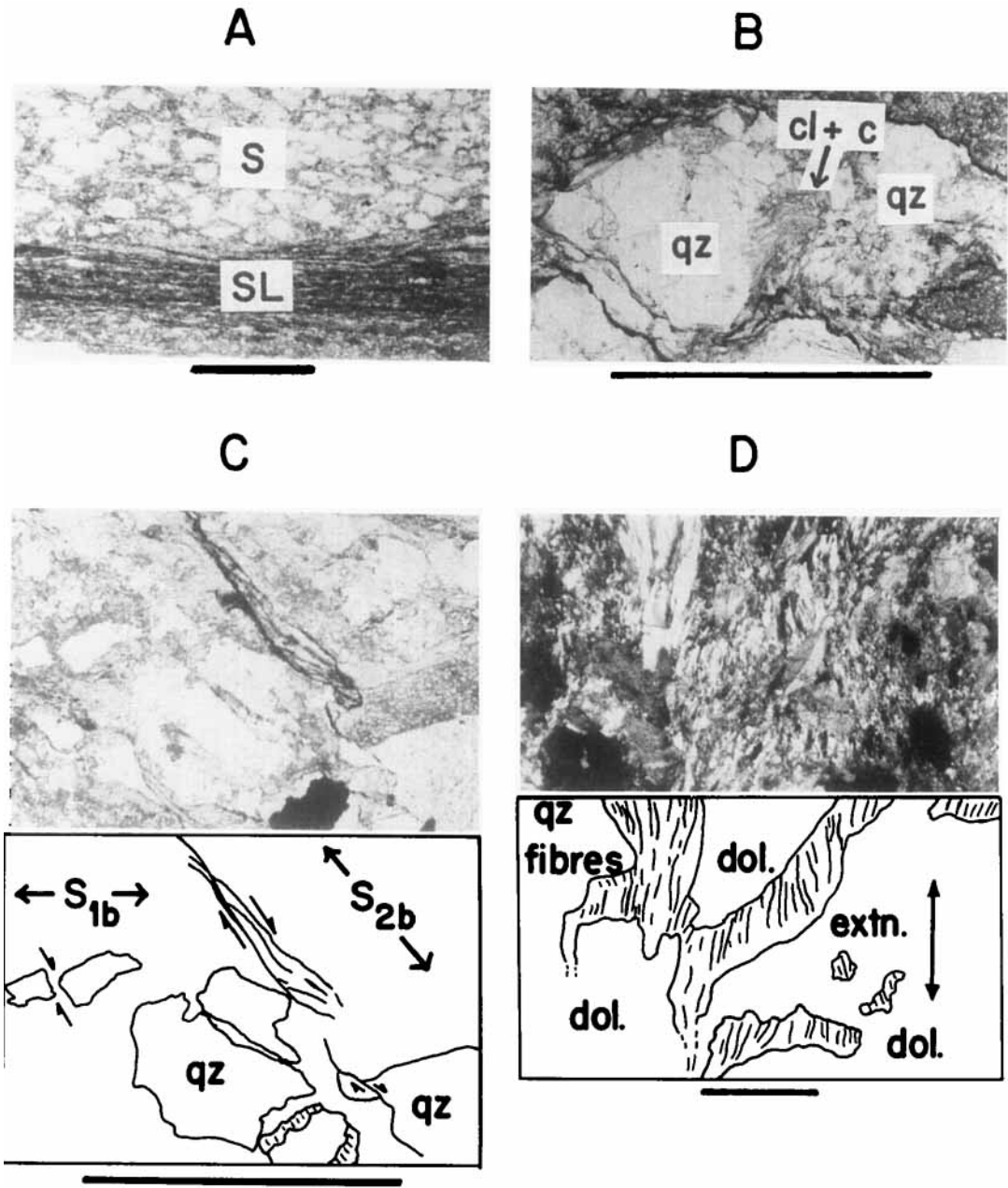
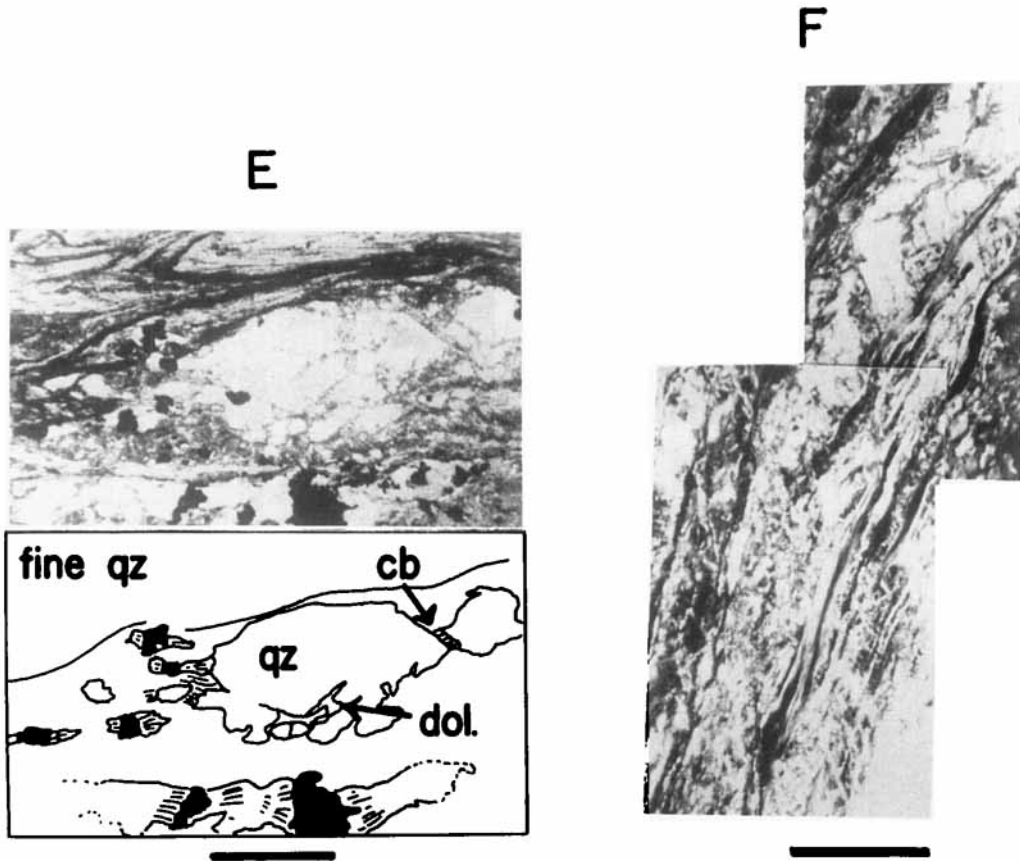


Fig. 5. Microscopic structural fabric elements in the upper package. All scale bars are 1 mm in length, PPL denotes plane polarized light, XPL denotes crossed polarizer and analyzer; details of localities can be obtained from the author.

- A. Holmesletfjella Fm. (BH1), south shore, M3548 PPL. Photomicrograph showing variation in the strength of cleavage development in siltstone (S) and slate (SL).  $S_{1b}$  trace is parallel to the scale bar.
- B. Holmesletfjella Fm. (BH1), south shore, M3529A PPL. Photomicrograph of chlorite and calcite (cl + c) growths between two parts of a fractured quartz (qz) grain.  $S_{1b}$  trace is parallel to the scale bar.
- C. Holmesletfjella Fm. (BH1), south shore, M3547B PPL. Sketch and photomicrograph of extensional crenulation cleavage ( $S_2$ ) developed adjacent to a large quartz grain.
- D. Orange-weathering dolostone (VOD), south shore, A012A XPL. Sketch and photomicrograph of 'tearing' fabric in the orange-weathering dolostone. Irregular regions of fibrous quartz occur throughout much of the rock, the long axes of the fibres are sub-parallel to each other.



E. Orange-weathering dolostone (VOD), south shore, M3572B PPL. Sketch and photomicrograph of rootless microfolds developed in very fine-grained quartz within the orange-weathering dolostone. Also shown are numerous pyrite grains (solid black in sketch) with long and complex quartz fibre growth. Large, recrystallized quartz (qz) grains have become fractured, and the fractures have filled with carbonate (cb), probably calcite. Dolomite has replaced part of the quartz grains and the calcite vein filling.

F. Orange-weathering dolostone (VOD), south shore, A012A XPL. Photomicrograph showing ribbon quartz developing from coarsely crystalline quartz in the orange-weathering dolostone.

Small amplitude open folds with approximately EW axial trends and gently SSW dipping axial surfaces deform both  $S_{1a}$  and  $S_{2a}$  and occur sporadically throughout the western exposures of the lower package ( $S_{3a}$  and  $F_{3a}$ , Fig. 1).

### Upper package

Bedding,  $S_{0b}$ , is distinguishable throughout the Bullbreen Group. Bed thicknesses vary from a few 10s of mm in the slates and silts to 5 m in the conglomerates.  $S_{0b}$  is usually manifest as a grain size and clay-mineral-content variation (Fig. 5A).

Cleavage,  $S_{1b}$ , is sub-parallel to the axial planes of tight folds developed in  $S_{0b}$ ; a bedding-cleavage intersection lineation,  $L_{1b}$ , is parallel to the axes of these folds.  $S_{1b}$  is primarily the result of pressure-

solution processes, and is marked by seams of accumulated pressure-insoluble material such as white mica, carbon and finely disseminated pyrite (Fig. 5A). Other components contribute to  $S_{1b}$ : micro-cracks in the larger quartz and dolomite grains (usually at high angles to  $S_{1b}$  and the inferred maximum extension direction, Fig. 5B), ductile flow of calcite clasts, pressure fringe overgrowths of calcite, quartz and chlorite, and calcite-filled crack-seal veins. An extensional renulation cleavage developed around competent grains during the  $S_{1b}$ -forming event (Fig. 5C). Sedimentary structures such as graded bedding, cross-bedding, flame structures and sole marks provide facing directions at many localities.

Major fold vergence in the Bullbreen Group is to the north. Minor fold and cleavage vergence

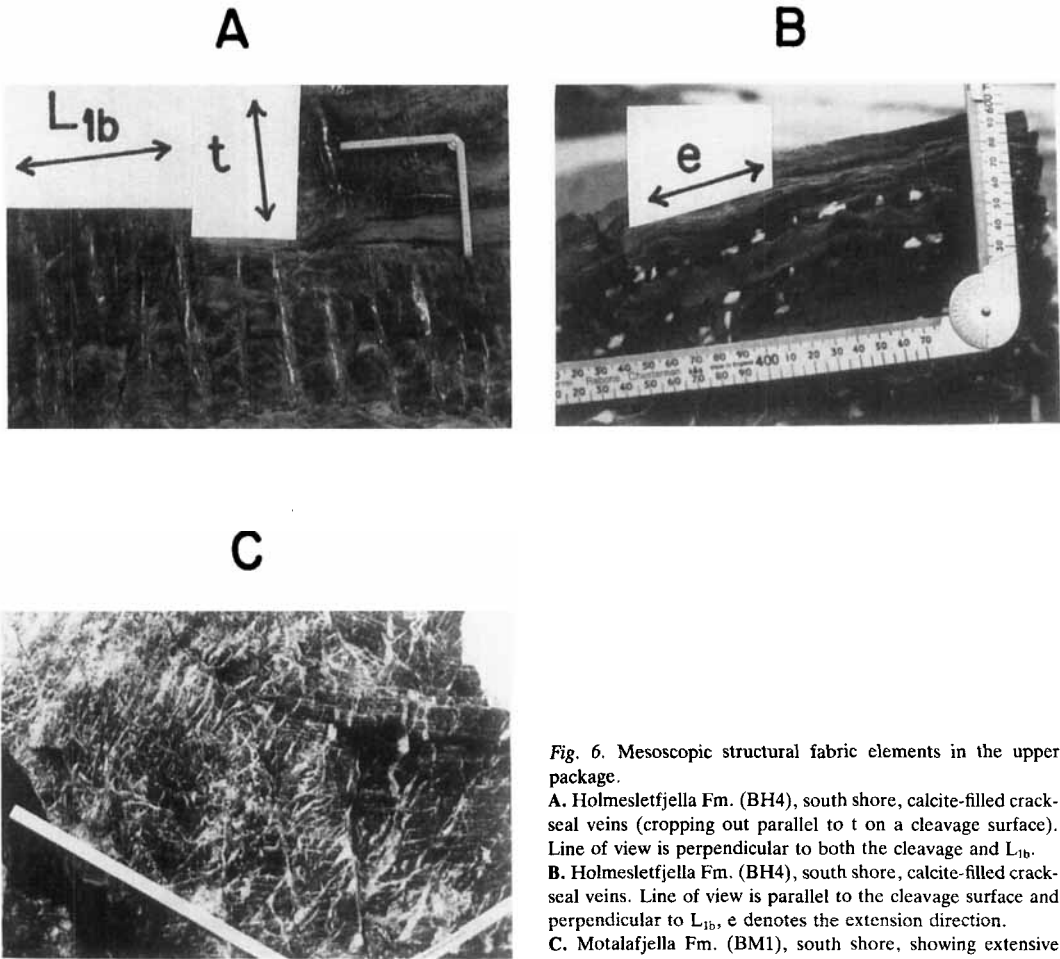


Fig. 6. Mesoscopic structural fabric elements in the upper package.

**A.** Holmesletfjella Fm. (BH4), south shore, calcite-filled crack-seal veins (cropping out parallel to  $t$  on a cleavage surface). Line of view is perpendicular to both the cleavage and  $L_{1b}$ .  
**B.** Holmesletfjella Fm. (BH4), south shore, calcite-filled crack-seal veins. Line of view is parallel to the cleavage surface and perpendicular to  $L_{1b}$ ,  $e$  denotes the extension direction.  
**C.** Motalafjella Fm. (BM1), south shore, showing extensive calcite veining.

variations are shown in Fig. 7A. Throughout most of the Bullbreen Group outcrop, facing direction is to the north. However, north and east of the Bullbreen glacier there is a small area (locality Y, filled circle, Map B, Fig. 1) in which the facing is reversed to a southerly direction (Fig. 7A).

$S_{1b}$  generally dips gently to the SW, and  $L_{1b}$  plunges gently west (sub-areas A, C2, C3 and D, Fig. 4). Poles to  $S_{0b}$  show a great-circle girdle pattern with a pole plunging gently to the west, consistent with  $L_{1b}$  (Fig. 4). However, on the eastern slopes of Thorkelsenfjella the orientation of  $S_{1b}$  is altered so that it dips gently to the SE, and  $L_{1b}$  plunges gently to the SE and east (compare sub-area C1 with D1 and D2, Fig. 4). A similar, but less severe change occurs in western Ankerfjella (compare sub-area A with D1 and D2, Fig. 4).

On the southwestern slopes of Holmesletfjella a locally developed kinking deforms both  $S_{0b}$  and  $S_{1b}$ . Kink zones are sub-horizontal with axes approximately NNW to SSE. Associated with this deformation is a crenulation cleavage with orientations that are sub-vertical (parallel to the short limb of kink folds) or sub-horizontal (parallel to the axial surface of kink folds).

Veins containing sigmoidal fibrous calcite are common features of the slates and siltstones in the Bullbreen Group. They are 5–10 mm thick quasi-planar veins spaced 50–100 mm apart and orientated perpendicularly to  $L_{1b}$  with fibre long axes sub-parallel to  $L_{1b}$  (Figs. 6A and B). A 3–4 m thick limestone near the base of the Bullbreen Group is heavily veined with calcite at many localities on the north slopes of Bulltinden (Fig. 6C).

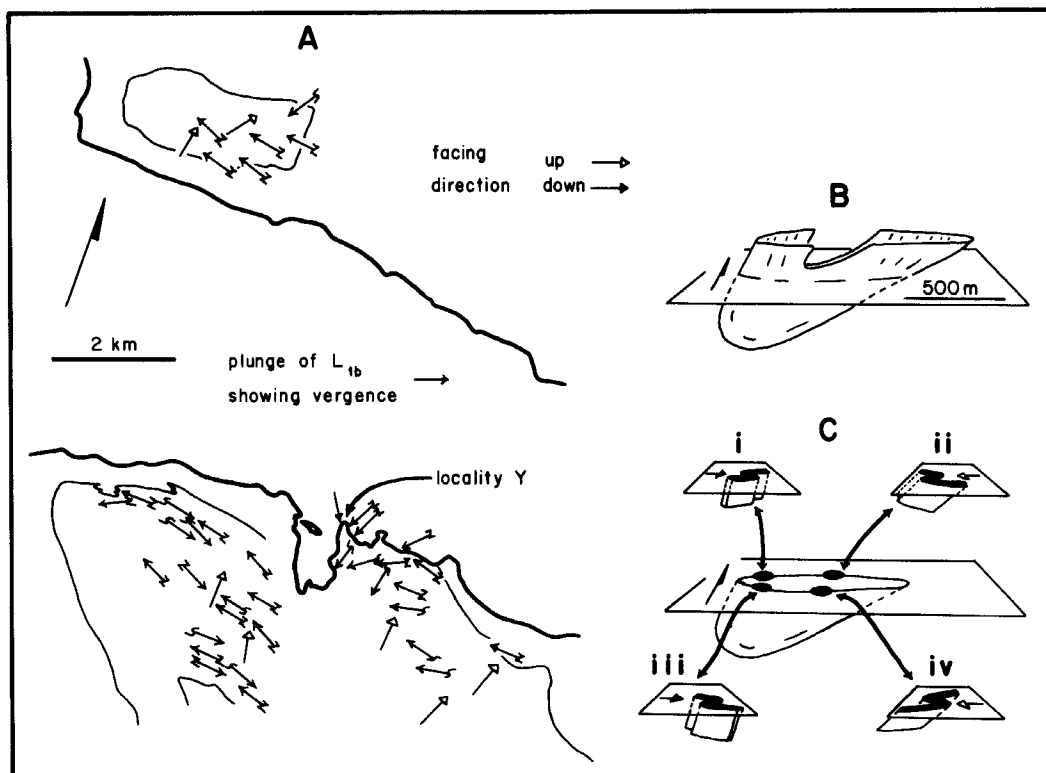


Fig. 7.

A. Map showing the facing and vergence relationships in the upper package. Note the downward, south-facing area at locality Y.  
 B. A fold to explain the facing and vergence relationships shown in A.  
 C. At locality Y the situation is as shown in III, situations II and IV occur to the east-northeast and south of Y, respectively. Situation I is not found.

### Orange-weathering dolostone

The unconformity between the Vestgötabreen Complex and the base of the Bullbreen Group is marked by a massive, orange-weathering dolostone (Ohta et al. 1984; Kanat & Morris 1988). Tectonic slices of this rock are found beneath the Bullbreen Group at many localities, even when other representatives of Vestgötabreen are absent. 'Tearing' structures similar to those found in the lower package are common, although the fibre growths are usually quartz (Fig. 5D). Rootless microfolds occur, and at some localities mylonitic textures have developed (Figs. 5E and F). Although not readily visible in exposure, a moderate to strong tectonic fabric is present, delineated by selvages of chlorite and mariposite, irregular quartz overgrowths, seams

of pressure insoluble material and extremely elongate quartz-grain shapes. Replacement of deformed quartz by coarse-grained dolomite, now deformed, is commonly observed (Fig. 5E).

### Inferred large-scale structures

#### *Lower package*

1.5 km east of Gaffelbreen, on the north shore, the Alkhorn limestone unit is in contact with a mafic sill. The western margin of the sill is marked by a 200 m wide zone in which are exposed vesicular mafic lava flows, lapilli tuffs, agglomerates and silicified limestone, all dipping steeply westwards. These are slivers of the volcanic unit within the Løvliebreen Formation and the meta-

morphic aureole of the sill. The sill itself is exposed along the shore for a distance of 0.8 km, and within it an igneous differentiation layering dips gently westwards (Gron 1984). East of this, the Alkhorn limestone unit lies above the Løvliebreen quartzite-slate unit, and the angular discordance between structural fabric elements above and below this contact indicates a thrust. A steeply dipping reverse fault (thrust ramp) marks the western end of the sill and a gently dipping thrust emplaces the banded carbonate unit over the mafic sill and the quartzite-slate unit (see cross section, Fig. 1).

In Ankerfjella (north shore) and along the raised beaches west of the Bullbreen glacier (south shore) a slice of Alkhorn limestone is directly overlain by the Haaken Formation diamictite. At the western end of Ankerfjella the total thickness of the Alkhorn limestone unit is 30 m, in the ridge south and east of Ankerbreen it is approximately 100 m thick, whereas in the ridge north and west of Ankerbreen it has an outcrop width of more than 1 km and it includes a number of tightly refolded folds. The contact between the Haaken diamictite and Alkhorn limestone is not deformed by these folds, and it clearly cross-cuts structures within the Alkhorn. The contact is inferred to be a thrust, post-dating the folds, along the base of Ankerfjella, steepening into a thrust ramp through Ankerbreen, and emplacing the Haaken diamictite over the Alkhorn limestone. An exactly analogous structure exists on the south shore, but the level of erosion and the presence of the Bullbreen glacier prevent good exposure of the contact.

At locality X (Map A, Fig. 1),  $F_{1a}$  z-folds are folded around a tight  $F_{2a}$  fold without changing vergence. The Løvliebreen volcanic unit is folded with the Alkhorn limestone and shows a fold closure 250 m northwest of X. This implies the existence of a recumbent  $F_{1a}$  synform, with a gently west-dipping axial surface and an approximately horizontal NS axis, which has been refolded about more steeply west-dipping axial surfaces. Enclosing this structure to the west and folded with the Alkhorn limestone is the Løvliebreen sandstone-phyllite unit (cross section, Fig. 1). Refolded folds in the Alkhorn limestone can also be identified in the ridge north and west of Ankerbreen, and similar, but less well-exposed, structures are found on the south shore.

At the western limit of exposure of the lower package all structural fabric elements are up-

turned to the west so that dips and plunges are to the east (sub-area C1, Fig. 4). This is particularly marked in Thorkelsenfjella and on the shore north of this ridge. Here, lower package rocks attain an almost vertical dip and their western margin abuts against a zone of strong deformation which contains tectonic slices of the Haaken Formation and Vestgötåbreen Complex rocks (Kanat & Morris 1988). This zone of deformation trends NW-SE, it separates the rocks described here from Carboniferous rocks and diamictite horizons to the south and west and it follows the trend of the southwestern limit of the Vestgötåbreen Complex. The sense of reorientation of structures within both the lower and upper packages indicates that the zone was most recently active as a west-dipping, reverse, oblique slip fault.

The orange-weathering dolostone unit does not contain bedding, it is highly altered and it has locally developed mylonitic textures. Above the dolostone, rocks of the Bullbreen Group contain no obvious discontinuity, although a limestone (Motalafjella limestone) band is heavily veined with calcite. The lower boundary of the dolostone is juxtaposed with the Haaken and Alkhorn Formations and the Vestgötåbreen Complex. There are marked differences in orientations of structural fabric elements between the rocks of the upper and lower packages (compare, for example,  $L_{1b}$  and  $L_{1a}$  orientations in Fig. 4). The dolostone is interpreted as a zone of hydrothermal alteration developed at the unconformity between the Bullbreen Group and the Vestgötåbreen Complex (Ohta et al. 1984), which acted as the locus for differential movement between the upper and lower packages.

### Upper package

In Bulltinden there occurs an asymmetrical, NNE-facing synformal syncline with a WNW to ESE trending axis and gently south-dipping axial surface. This is inferred from the occurrence of the basal sequence of the Bullbreen Group both on the northern slopes of Bulltinden and at its southern extremity. Vergence changes are consistent with this interpretation. Holmesletfjella are occupied by a fold similar to that of Bulltinden; this is inferred from vergence and younging direction changes and from the repetition of distinctive conglomeratic horizons on the northeastern and southwestern slopes of the ridge. A continuation of this structure can be seen as a

closure within the Bullbreen Group in Motalfjella (Kanat 1986; Ohta pers. comm.).

At locality Y (Figs. 1 and 7A) the facing direction is to the south-east, elsewhere in the Bullbreen Group outcrop, the facing is to the north. The vergence at this locality is z-type. This relationship between facing and vergence can be explained by a structure as shown in Figs. 7B and C. One possible cause of such a structure is a NS trending, westerly dipping reverse fault through the Bullbreen glacier, with movement on the fault having caused rotation of pre-existing structures in the footwall. This fault would also explain the higher elevation of the Bullbreen Group west of the glacier as compared to east of the glacier (a difference of 50–100 m). It is also consistent with structures mapped by Hjelle et al. (1979), Ohta (1979) and Kanat (1986).

At the western limit of the Bullbreen Group outcrop along the eastern slopes of Thorkelsenfjella (sub-area C1, Fig. 4) and at the western end of Ankerfjella the gentle westerly plunge of  $L_{1b}$  and south-southwesterly dip of  $S_{1b}$  are reorientated to easterly plunges and dips. This is caused by the same fault that reorientates structural features in the lower package.

## Summary

The oldest deformation features in the lower package,  $S_{1a}$  and  $S_{2a}$ , together with associated folds and refolds, resulted from approximately EW compression. Interference patterns produced by the two fold phases are Type 3 (Ramsay 1967). First formed folds had gently west-dipping axial surfaces with almost horizontal NS axes, and the second phase folds were almost coaxial with more steeply west-dipping axial surfaces. Such a pattern creates lithological interbanding which can resemble sedimentary transition sequences, and greatly increases the apparent thickness of stratigraphic units. One of the best developed areas of Type 3 interference patterns so far mapped in the St. Jonsfjorden area is the southern slope of Lowzowfjella (Fig. 1). It is in precisely this area that previous workers have described the greatest thickness of the Alhorn Formation and the occurrence of gradational contacts characterized by lithological alternations (e.g. Waddams 1983). Superimposed on these early structures are locally developed EW trending kinks and easterly directed thrusts.

The upper package contains evidence for two principal deformation events. The first occurred during approximately NS compression and concomitant dextral strike-slip along the basin margins (Ratliff et al. 1988), and produced  $S_{1b}$ , associated north verging folds and northerly directed thrusting. A second major event involved easterly directed thrusting and/or reverse faulting.

## Discussion

A precise chronology for, and the inter-relationship between these various deformation events is by no means clear from the available data. However, the first fold phase in the lower package is most probably Caledonian in age, given that the Haaken diamictites are late Proterozoic, and may well be approximately coeval with the principal metamorphic cooling age of 460–470 Ma obtained from the Vestgötabreen high-pressure schists (Ohta & Dallmeyer 1986). The second phase of folding in the lower package is more problematic. It is tempting to correlate it with the easterly thrusting event common to both packages. If this were true, however, the intervening NS compression responsible for the upper package main deformation should be clearly distinguishable between the two lower package fold phases. Minor EW kinking in the lower package is the only evidence for a NS compressive event, and this is superimposed on both NS trending fold phases. In addition, it is difficult to envision two deformation phases within one package, both involving extensive pressure solution, separated by a deformation phase characterized by kinking and chevron style folds, that survived the second pressure solution event. In the absence of other evidence the most logical chronology for the two NS trending, interfering fold phases in the lower package is that they are both Caledonian.

There remains the enigma of the principal deformation experienced by the upper package: how could such a significant event produce only minor folding in the lower package? Two explanations can be offered: 1) At the time of this deformation (probably 400 Ma) (Ohta & Dallmeyer 1986; Ohta & Dallmeyer pers. comm.) the Bullbreen Group was perhaps not more than 20 Ma old (Scrutton et al. 1976), whereas the lower package was already deformed, metamorphosed to low greenschist facies, and largely

dewatered. 2) The cause of this deformation event was probably NS compression activating a NW-SE trending strike-slip fault that marked the SW limit of the Bullbreen basin; the resultant interaction between dextral strike-slip and compression was limited to a narrow zone along this fault (Ratliff et al. 1988).

Finally, the easterly directed thrusting is best correlated with the west Spitsbergen Orogeny in the early Tertiary; the EW compression, sense of thrust motion and general style of deformation are all consistent with other areas in western Spitsbergen (Harland & Horsfield 1974).

*Acknowledgements.* – Financial and logistical support was provided for this project by National Science Foundation grant DPP-8107663, Wayne State University in Detroit, Cambridge Spitsbergen Expeditions, Norsk Polarinstittutt and the University of Texas at San Antonio. I am indebted to Leslie Kanat, Jay Ague, Daria Walniuk, Shelley Gron, Bob Ratliff and Matthew Dodt, without whose able assistance and informed comments this work would not have been possible. Campbell Craddock and Yoshihide Ohta made substantial improvements to an early manuscript of this paper.

## References

- Armstrong, H. A., Nakrem, H. A. & Ohta, Y. 1986: Ordovician conodonts from the Bulltinden Formation, Motalafjella, central-western Spitsbergen. *Polar Research 4 n.s.*, 17–23.
- Bell, A. M. 1981: Vergence: an evaluation. *Journal of Structural Geology 3*, 197–202.
- Birkenmajer, K. 1981: The geology of Svalbard, the western part of the Barents Sea, and the continental margin of Scandinavia. Pp. 265–329 in Nairn, A. E. M. (ed.): *The ocean basins and margins 5: The Arctic Ocean*.
- Gron, S. A. 1984: *A study of the igneous horizons in the St. Jonsfjorden and Løvliebreen Groups in west Spitsbergen*. M.S. Thesis, Wayne State University, Detroit. 242 pp.
- Hambrey, M. J. 1983: Correlation of Late Proterozoic tillites in the North Atlantic region and Europe. *Geological Magazine 120*, 209–232.
- Harland, W. B. & Horsfield, W. T. 1974: West Spitsbergen Orogen. Pp. 747–755 in Spencer, A. M. (ed.): *Mesozoic-Cenozoic Orogenic Belts, Data for Orogenic Studies. Special Publication of the Geological Society, London, 4*.
- Harland, W. B., Horsfield, W. T., Manby, G. M. & Morris, A. P. 1979: An outline pre-Carboniferous stratigraphy of central western Spitsbergen. *Norsk Polarinstittutt Skrifter 167*, 119–144.
- Hjelle, A., Ohta, Y., Winsnes, T. S. 1979: Hecla Hoek rocks of Oscar II Land and Prins Karls Forland, Svalbard. *Norsk Polarinstittutt Skrifter 167*, 145–169.
- Horsfield, W. T. 1972: Glaucophane schists of Caledonian age from Spitsbergen. *Geological Magazine 109*, 29–36.
- Kanat, L. H. 1986: *Aspects of the geology of south west Oscar II Land, Spitsbergen*. Ph.D. Thesis, University of Cambridge. 203 pp.
- Kanat, L. H. & Morris, A. P. 1988: A working stratigraphy for central western Oscar II Land, Spitsbergen. *Norsk Polarinstittutt Skrifter 190* (in press).
- Kowallis, B. J. & Craddock, C. 1984: Stratigraphy and structure of the Kapp Lyell diamictites (upper Proterozoic), Spitsbergen. *Geological Society of America Bulletin 95*, 1293–1302.
- Ohta, Y. 1979 Blue schists from Motalafjella, western Spitsbergen: *Norsk Polarinstittutt Skrifter 167*, 171–217.
- Ohta, Y., Hiroi, Y. & Hirajima, T. 1984: Additional evidence for pre-Silurian high-pressure metamorphic rocks on Spitsbergen. *Polar Research 1 n.s.*, 215–218.
- Ohta, Y., Hirajima, T. & Hiroi, Y. 1986: Caledonian high-pressure metamorphism in central western Spitsbergen. *Geological Society of America Memoir 164*, 205–216.
- Ohta, Y. & Dallmeyer, R. D. 1986: Polyorogenic evolution of the Svalbard Caledonides and tectonic correlations with northern Grønland and Arctic Canada. *Geological Society of America, Abstracts with Programs 18*, 710.
- Platt, J. P. & Vissers, R. L. M. 1980: Extensional structures in anisotropic rocks. *Journal of Structural Geology 2*, 397–410.
- Ramsay, J. G. 1967: *Folding and fracturing of rocks*. McGraw-Hill. 568 pp.
- Ratliff, R. A., Morris, A. P. & Dodt, M. E. 1988: Interaction between strike-slip and thrust-shear: deformation of the Bullbreen Group, central-western Spitsbergen. *Journal of Geology 96*, 339–349.
- Scrutton, C. T., Horsfield, W. T. & Harland, W. B. 1976: A Silurian fauna from western Spitsbergen. *Geological Magazine 113*, 519–523.
- Shackleton, R. M. 1957: Downward-facing structures of the Highland Border. *Quarterly Journal of the Geological Society, London 113*, 361–397.
- Turner, F. J. & Weiss, L. E. 1963: *Structural Analysis of Metamorphic Tectonites*. McGraw-Hill. 545 pp.
- Waddams, P. 1983: The late Precambrian succession in north-west Oscar II Land, Spitsbergen. *Geological Magazine 120*, 233–252.
- Woodcock, N. H. & Naylor, M. A. 1983: Randomness testing in three-dimensional orientation data. *Journal of Structural Geology, 5*, 530–548.
- Weiss, L. E. 1953: Tectonic features of the Hecla Hoek to the south of St. Jonsfjorden, Vestspitsbergen: *Geological Magazine 90*, 273–286.